GASEOUS FLOWS IN MICROCHANNELS

I.A. Graur*, J.G. Méolans* and D.E. Zeitoun*

*Universite de Provence - Ecole Polytechnique Universitaire de Marseille, UMR CNRS 6595, 5 rue Enrico Fermi, 13453 Marseille, France

Abstract. The objective of this study is to broaden the fundamental understanding of the emerging field of microfluidics especially in a long channel. The quasi gasdynamic (QGD) equations, originally developed on the basis of a kinetical model are used for numerical and analytical simulation. A two-dimensional analysis of the QGD equations with a first order slip velocity boundary conditions demonstrates that both compressibility and rarefied effects are present in long microchannels. Analytical solutions for the pressure and the velocity profiles are derived from the quasi gasdynamic equations by undertaking perturbation expansions according to a small parameter ε (the height-to-length ratio of the channel) and using the isothermal flow assumption. The deduced expression for the mass flow rate is similar to the analytical expression obtained from the Navier-Stokes equations with a second order slip boundary condition and gives results in agreement with the measurements. The effects of the rarefaction and of the compressibility on pressure distributions are analyzed. The analytical expression of the pressure predicts accurately the measured pressure distribution. The Knudsen numbers calculated at the exit of the channel and based on the channel height vary from 10^{-3} to 0.4. The comparisons of analytical and numerical solutions confirm the validity of the analytical approach.

INTRODUCTION

A systematic research effort in micro mechanics devices started in the late 1980's. The characteristic length scale of these devices is less than 1 mm. Then, even at the atmospheric conditions, the ratio of the mean-free path to the characteristic dimension can not be neglected and in the flow dynamic associated with MEMS the rarefied gas phenomena become apparent. In the present study an analytical and numerical investigation of slightly rarefied gaseous flows through long microchannels is undertaken. Analytical expressions of the streamwise mass flow rate, pressure and velocity profiles are derived from the quasi gasdynamic (QGD) equations [1] through perturbation expansions according to ε (the height-to-length ratio of the channel) under the isothermal flow assumption.

We obtain a mass flow rate expression similar to that previously derived from the Navier-Stokes (NS) equations associated to a second order slip boundary conditions. This expression gives results in agreement with the measurements. Regarding this point, we must especially mentioned a study [2] based on the quasi hydrodynamic (QHD) equations written out for a plane stationary isothermal gas flow in a long channel; since the QHD and QGD systems are both founded on the same basic concept, even if involving different closures of the conservation equation system [1], thus an analytical mass flow rate formulation was given in [2] very close to that presented in this paper. Furthermore we derive from our perturbation method the pressure and the velocity profiles at ε zero order. The analytical expression of the pressure predicts accurately the measured pressure distribution [3]. The effect of the rarefaction and of the compressibility on the pressure and on the velocity distributions are pointed out and discussed. Otherwise the numerical calculations based on the full system of the QGD equations were carried out for different sizes of the microchannels and for various gases. The agreement between analytical and numerical results confirms the validity of the analytical approach.

QGD EQUATIONS: SIMPLIFIED ISOTHERMAL FORM

The QGD equations are a gasdynamic system closed with a special choice of mass flux vector, shear-stress tensor and heat flux vector, determined by means of time-space averaging (instead of space averaging for the Navier-Stokes equations) for the gasdynamic quantities ρ, u_i and p [1]. The general form of the QGD system is presented in [1],

CP762, *Rarefied Gas Dynamics: 24th International Symposium,* edited by M. Capitelli

Report Documentation Page

Form Approved
OMB No. 0704-0188

1. REPORT DATE	2. REPORT TYPE	3. DATES COVERED
13 JUL 2005	**N/A**	**-**

4. TITLE AND SUBTITLE	5a. CONTRACT NUMBER
Gaseous Flows in Microchannels	5b. GRANT NUMBER
	5c. PROGRAM ELEMENT NUMBER
6. AUTHOR(S)	5d. PROJECT NUMBER
	5e. TASK NUMBER
	5f. WORK UNIT NUMBER
7. PERFORMING ORGANIZATION NAME(S) AND ADDRESS(ES) **Universite de Provence - Ecole Polytechnique Universitaire de Marseille, UMR CNRS 6595, 5 rue Enrico Fermi, 13453 Marseille, France**	8. PERFORMING ORGANIZATION REPORT NUMBER
9. SPONSORING/MONITORING AGENCY NAME(S) AND ADDRESS(ES)	10. SPONSOR/MONITOR'S ACRONYM(S)
	11. SPONSOR/MONITOR'S REPORT NUMBER(S)

12. DISTRIBUTION/AVAILABILITY STATEMENT
Approved for public release, distribution unlimited

13. SUPPLEMENTARY NOTES
See also ADM001792, International Symposium on Rarefied Gas Dynamics (24th) Held in Monopoli (Bari), Italy on 10-16 July 2004.

14. ABSTRACT

15. SUBJECT TERMS

16. SECURITY CLASSIFICATION OF:			17. LIMITATION OF ABSTRACT	18. NUMBER OF PAGES	19a. NAME OF RESPONSIBLE PERSON
a. REPORT **unclassified**	b. ABSTRACT **unclassified**	c. THIS PAGE **unclassified**	**UU**	**6**	

[4]. The 2-D flow is considered to be isothermal, therefore the energy equation is not taken into account in the present analysis.

The variables are non-dimensioned in the following manner: the streamwise coordinate x by the channel length L; the wall-normal coordinate y, by the channel height H, the velocities u and v are normalized by the velocity u_o on the axis at the channel exit (the subscript "o" refers to the outlet conditions); the density and the viscosity coefficient by the appropriate outlet values ρ_o and μ_o. The channel height-to-length ratio ε will be small compared to unity: $\varepsilon = H/L, \varepsilon \ll 1$. The choice of the pressure normalization is based on the following reason: the pressure changes due to inertia indeed are very small at small Mach numbers (that is the case in microflows [5]). Thus in a long microchannel these pressure changes along the channel are mostly due to viscous effects. Therefore we suppose that they are proportional to the viscous forces: $\frac{\Delta p}{L} \sim \mu \frac{\partial^2 u}{\partial y^2}$, that leads to choose as the referenced pressure $u_o L \mu_o / H^2$ for the non-dimensionalisation. Moreover, in the various experiments investigated hereafter the pressure change is of the same order as the pressure itself: so, the non-dimensional pressure is guaranteed to be of zero order in ε as the others non-dimensional parameters are. Now we expand the velocities, the density and the pressure in powers of ε up to the first order:

$$\tilde{u} = \tilde{u}_0 + \varepsilon \tilde{u}_1, \qquad \tilde{v} = \varepsilon \tilde{v}_1, \qquad \tilde{\rho} = \tilde{\rho}_0 + \varepsilon \tilde{\rho}_1, \qquad \tilde{p} = \tilde{p}_0 + \varepsilon \tilde{p}_1, \tag{1}$$

and we substitute the expressions (1) into the non-dimensional system as it was fulfilled in similar analysis of the NS equations [6]. Disregarding the flows of $O(1/\varepsilon)$ Reynolds numbers (where $Re = \rho_o u_o H / \mu_o$, evaluated in the outlet conditions) analyzed in the boundary layer theory [7], the remaining flow regimes characterized by $Re \sim O(1)$ and $O(\varepsilon)$ are regimes classified as microflows and may be appropriately treated by the current perturbation analysis. Multiplying the y-momentum equation by the factor $\varepsilon^2 Re$ and keeping the ε zero order terms we obtain (omitting from now the zero subscript) $\partial \tilde{p} / \partial \tilde{y} = 0$, thus the pressure is expected to be uniform across any section of the channel. We use this result and the isothermal flow assumption (so the temperature and viscosity coefficient are constant), and we neglect the terms of ε/Re, 1 and $1/Re$ order against the term of $1/(\varepsilon Re)$ order. Then multiplying the x-momentum equation by εRe we obtain at zero order

$$\frac{\partial \tilde{p}}{\partial \tilde{x}} = \tilde{\mu} \frac{\partial^2 \tilde{u}}{\partial \tilde{y}^2}. \tag{2}$$

We can remark that the momentum equations are the same as those obtained with the NS system [6], [8].

Then, the boundary conditions for the equation (2) are the following: the symmetry condition on the axis and the slip velocity boundary condition on the solid wall, that in the isothermal case reads [9]

$$u_s = \sigma_p \frac{\mu}{p} v_m \left(\frac{\partial u}{\partial y} \right)_w, \tag{3}$$

where $v_m = \sqrt{2 \mathscr{R} T_w}$ is the most probable molecular velocity at the surface temperature T_w; σ_p is the slip velocity coefficient. The value of the slip velocity coefficient σ_p suggested by Maxwell is $\sigma_p^M = 0.5 \sqrt{\pi} (2 - \alpha)/\alpha$, where α is the part of the molecules reflected diffusively. In the case of the full accommodation the coefficient σ_p^M is equal to 0.886. But in this article, unless advised otherwise, we will use for the QGD equations the velocity slip coefficient $\sigma_p^K = 1.012$, given by Kogan [10] under the full accommodation assumption. This value is close to the one proposed by Sharipov [9] $\sigma_p^S = 1.0$ in the case of the diffuse gas-surface interaction.

Furthermore the mean free path, as a function of macroscopic parameters, is usually written as $\lambda = k_\lambda \mu / p \sqrt{\mathscr{R} T}$. In this equation the coefficient k_λ depends on the molecular interaction model. For the HS model the Chapman formula [11] leads to $k_\lambda = \sqrt{\pi/2}$. For the present QGD equations we will use, unless advised otherwise, $k_\lambda = A(\omega) = \frac{2(7-2\omega)(5-2\omega)}{15\sqrt{2\pi}}$, the expression deduced by Bird [12] for the VHS model; the coefficient $A(\omega)$ depends only on the type of the gases. The slip velocity is related to the mean free path and to the velocity gradient through the expression:

$$u_s = \sigma_p \frac{\sqrt{2}}{k_\lambda} \lambda \left(\frac{\partial u}{\partial y} \right)_w = K_{slip} \lambda \left(\frac{\partial u}{\partial y} \right)_w, \quad \text{or in non-dimensional form} \quad \tilde{u}_s = K_{slip} Kn \left(\frac{\partial \tilde{u}}{\partial \tilde{y}} \right)_w, \quad K_{slip} = \sigma_p \frac{\sqrt{2}}{k_\lambda}, \tag{4}$$

where $Kn = \lambda / H$ is the local Knudsen number and K_{slip} is a non-dimensional coefficient.

Using the symmetry condition and the slip-flow boundary condition (4) the simplified x-momentum equation (2) can be integrated twice with respect to y, leading to:

$$\tilde{u}(\tilde{x}, \tilde{y}) = -\frac{1}{8\tilde{\mu}} \frac{d\tilde{p}}{d\tilde{x}} \left(1 - 4\tilde{y}^2 + 4 K_{slip} Kn \right). \tag{5}$$

The same form of the velocity distribution was obtained using a first order boundary condition associated to the Navier-Stokes equations in [6], [8]. Note that the streamwise velocity depends explicitly upon the wall-normal (y) direction and also on the streamwise (x) direction via the local Knudsen number.

We can now calculate the mass flow through the channel for given inlet and outlet pressures. Neglecting the terms of order equal or superior to $O(\varepsilon)$ in the non-dimensional form of the QGD mass flux, we obtain:

$$\tilde{J}^x = \tilde{\rho}\tilde{u} - \frac{\varepsilon}{Re}\frac{\tilde{\mu}}{\tilde{p}}\frac{d\tilde{p}}{d\tilde{x}}. \tag{6}$$

In comparison with the mass flux given by the NS equations the QGD mass flux contains the additional term proportional to the streamwise pressure gradient. This term is kept at zero order assuming $Re \sim O(\varepsilon)$. Integrating the mass flux (6) across the channel, using the streamwise velocity (5) and the state equations, we obtain:

$$\tilde{J} = -\frac{1}{24\tilde{\mu}\tilde{T}}\frac{d\tilde{p}}{d\tilde{x}}\frac{\gamma Ma^2}{\varepsilon Re}\left(2\tilde{p} + 12K_{slip}k_\lambda\frac{\varepsilon}{\sqrt{\gamma}Ma}\tilde{\mu}\sqrt{\tilde{T}} + 24\frac{\varepsilon^2}{\gamma Ma^2}\frac{\tilde{\mu}^2\tilde{T}}{\tilde{p}}\right). \tag{7}$$

Integrating the mass flow rate (7) in the streamwise direction from 0 to 1 and expressing the local Knudsen number as $Kn = Kn_o\tilde{p}_o/\tilde{p}$, then using the mass flow conservation along the channel, we obtain finally a mass flow rate expression depending on the inlet and outlet pressure $\mathscr{P} = \tilde{p}_i/\tilde{p}_o$:

$$\tilde{J} = \frac{\tilde{p}_o^2}{24\tilde{\mu}\tilde{T}}\frac{\gamma Ma^2}{\varepsilon Re}\left(\mathscr{P}^2 - 1 + 12K_{slip}Kn_o(\mathscr{P}-1) + \frac{24}{k_\lambda^2}Kn_o^2\ln\mathscr{P}\right). \tag{8}$$

This relationship presents in fact the non-dimensional flow rate per width unit. Then the effects of the slip condition and of the QGD additional term in the mass flux appear more clearly dividing (8) by the mass flow rate deduced from the NS equations with no-slip condition (J_{NS}^{noslip}):

$$J_{QGD}/J_{NS}^{noslip} = 1 + 12K_{slip}Kn_o\frac{1}{\mathscr{P}+1} + \frac{24}{k_\lambda^2}Kn_o^2\frac{\ln\mathscr{P}}{\mathscr{P}^2-1}, \qquad J_{NS}^{noslip} = \frac{\tilde{p}_o^2}{24\tilde{\mu}\tilde{T}}\frac{\gamma Ma^2}{\varepsilon Re}\left(\mathscr{P}^2-1\right). \tag{9}$$

Moreover using the first order slip boundary condition with the NS equations, the mass flow expressed by [6], [8], [13] takes the form

$$J_{NS}^{slip1}/J_{NS}^{noslip} = 1 + 12K_{slip}Kn_o\frac{1}{\mathscr{P}+1}. \tag{10}$$

The last term of expression (9) (in Kn^2 order) is the additional term introduced by the QGD model in respect to the NS model (10), when both the models are used with the same first order boundary condition. As said in the introduction, this term is similar to that derived from QHD model in [2]: the two expressions differ only by the Schmidt number which appears in denominator of the Kn^2 term of QHD model. Note that in [2] comparing their results with the measurements the authors found an agreement in the $0.1 - 0.5\,Kn$ range.

Various expressions of second order slip boundary conditions were suggested by numerous authors [8], [13] to supplement the NS equations: so in [8] a second order boundary condition leads to the following mass flow rate

$$J_{NS_B}^{slip2}/J_{NS}^{noslip} = 1 + 12K_{slip}Kn_o\frac{1}{\mathscr{P}+1} - 12\frac{2-\alpha}{\alpha}Kn_o^2\frac{\ln\mathscr{P}}{\mathscr{P}^2-1}. \tag{11}$$

The authors [8] explained that the effect of the second order correction is to reduce the increase in mass flow rate due to the first order slip. On the contrary, implementing in the NS equations another second order boundary conditions [14], other authors [13] obtained a correction increasing the mass flow rate:

$$J_{NS_C}^{slip2}/J_{NS}^{noslip} = 1 + 12K_{slip}Kn_o\frac{1}{\mathscr{P}+1} + 27Kn_o^2\frac{\ln\mathscr{P}}{\mathscr{P}^2-1}, \tag{12}$$

and this expression seems to lead to results in agreement with the measurements of the authors.

In Fig. 1 a) are compared for helium flows:

- Three results obtained in the Navier-Stokes theoretical frame, utilizing respectively the expression (10) derived from the first order formula, the mass flow rate (11) coming from a second order slip condition [8] and the expression (12) constructed in [13] from another second order slip condition [14].

- The results obtained from the present analytical QGD treatment coupled to the first order slip condition which leads to expression (9).
- The corresponding experimental results [6].

These calculations and measurements concern helium streams through a $1.33\mu m$ deep rectangular microchannel and are obtained for the atmospheric outlet pressure and $Kn_o = 0.165$. In order to obtain significant comparisons we have firstly calculated the various theoretical mass flow rates with the same "slip parameters": i.e. $k_\lambda = \sqrt{\pi/2}$ and $\sigma_p = \frac{\sqrt{\pi}}{2}\frac{2-\alpha}{\alpha}$, and in any case a complete diffuse reflection. In these conditions the QGD approach agrees with the measurements slightly better than the other approaches (Fig. 1 a). Then we have plotted the QGD results calculated with our usual "slip parameters" ($k_\lambda = A(\omega)$, $\sigma_p^K = 1.012$) admitting again a complete diffuse reflection. One can see in Fig. 1 a, that the improvement is at the least of the same order when changing the slip parameters (k_λ, σ_p) as when changing the Knudsen number order of the continuum approach. Furthermore, the prevalent governing effects of the solid surface parameters appears clearly if noting that k_λ disappears from all the coefficients ($Kn_o K_{slip}$ and Kn_o/k_λ) in the previous mass flow rate expressions (9)-(12), while σ_p remains explicitly. So, the reflection process at the wall exerts here a direct influence while the intermolecular forces act only through the viscosity coefficient, whatever the interaction model used in the gas.

STREAMWISE PRESSURE DISTRIBUTION AND VELOCITY PROFILES

By integrating the mass flow rate (7) in the streamwise direction from 0 to $\tilde{x}$ we obtain an implicit relation for the pressure distribution along the channel:

$$\left(\tilde{p}(\tilde{x}) + 6K_{slip}k_\lambda \frac{\varepsilon\tilde{\mu}\sqrt{\tilde{T}}}{\sqrt{\gamma}Ma}\right)^2 - \left(\tilde{p}_i + 6K_{slip}k_\lambda \frac{\varepsilon\tilde{\mu}\sqrt{\tilde{T}}}{\sqrt{\gamma}Ma}\right)^2 + 24\frac{\varepsilon^2}{\gamma Ma^2}\tilde{\mu}^2\tilde{T}\ln\frac{\tilde{p}(\tilde{x})}{\tilde{p}_i} = -24\tilde{x}\tilde{J}\tilde{\mu}\tilde{T}\frac{\varepsilon Re}{\gamma Ma}. \tag{13}$$

Accounting for $\tilde{p}(\tilde{x}) < \tilde{p}_i$, we expand the pressure logarithmic function in the Taylor series of pressure difference. If we truncate the above equation to retain only the terms of the first order in pressure difference, we obtain a simple explicit expression for the pressure distribution:

$$\frac{\tilde{p}(\tilde{x})}{\tilde{p}_o} = \sqrt{(\mathscr{P} + 6K_{slip}Kn_o)^2 - \tilde{x}F(\mathscr{P}) + \left(\frac{12}{\mathscr{P}}\frac{Kn_o^2}{k_\lambda^2}\right)^2 + \frac{24}{\mathscr{P}}\frac{Kn_o^2}{k_\lambda^2}\left(\mathscr{P} + 6K_{slip}Kn_o\right)} - \left(6K_{slip}Kn_o + \frac{12}{\mathscr{P}}\frac{Kn_o^2}{k_\lambda^2}\right),$$

$$F(\mathscr{P}) = \mathscr{P}^2 - 1 + 12K_{slip}Kn_o(\mathscr{P} - 1) + \frac{24}{\mathscr{P}}\frac{Kn_o^2}{k_\lambda^2}(\mathscr{P} - 1). \tag{14}$$

Using the expansion of the logarithmic function up to the second order terms, leads to a more accurate explicit expression of the pressure. The analytical expression obtained in [6] from the NS equations with the first order slip boundary conditions gives:

$$\tilde{p}(\tilde{x})/\tilde{p}_o = \sqrt{(\mathscr{P} + 6K_{slip}Kn_o)^2 - \tilde{x}\left(\mathscr{P}^2 - 1 + 12K_{slip}Kn_o(\mathscr{P} - 1)\right)} - 6K_{slip}Kn_o. \tag{15}$$

Comparing the last two expressions, it appears that, although both parabolic, the pressure distributions (14) and (15) present different curvatures along $\tilde{x}$. Furthermore if expanding the square root in Kn power only the Kn zero order terms would be the same in (14) and (15). As previously noted for the mass flow rates, the pressure profiles are independent of k_λ. On the other hand, in Fig. 1 b the analytical pressure distribution (14) is compared with pressure measurements [3], corresponding to a $1.2\mu m$ deep channel charged with nitrogen and exhausting to atmospheric conditions: the predicted pressure distribution is non linear and coincides very well with the measured values.

It may easily be proven from (14) that the curvature of the pressure distribution is negative, since

$$\frac{d\tilde{p}(\tilde{x})}{d\tilde{x}} = -\frac{F(\mathscr{P})}{2\sqrt{(\mathscr{P} + 6K_{slip}Kn_o)^2 - \tilde{x}F(\mathscr{P}) + \left(\frac{12}{\mathscr{P}}\frac{Kn_o^2}{k_\lambda^2}\right)^2 + \frac{24}{\mathscr{P}}\frac{Kn_o^2}{k_\lambda^2}\left(\mathscr{P} + 6K_{slip}Kn_o\right)}}. \tag{16}$$

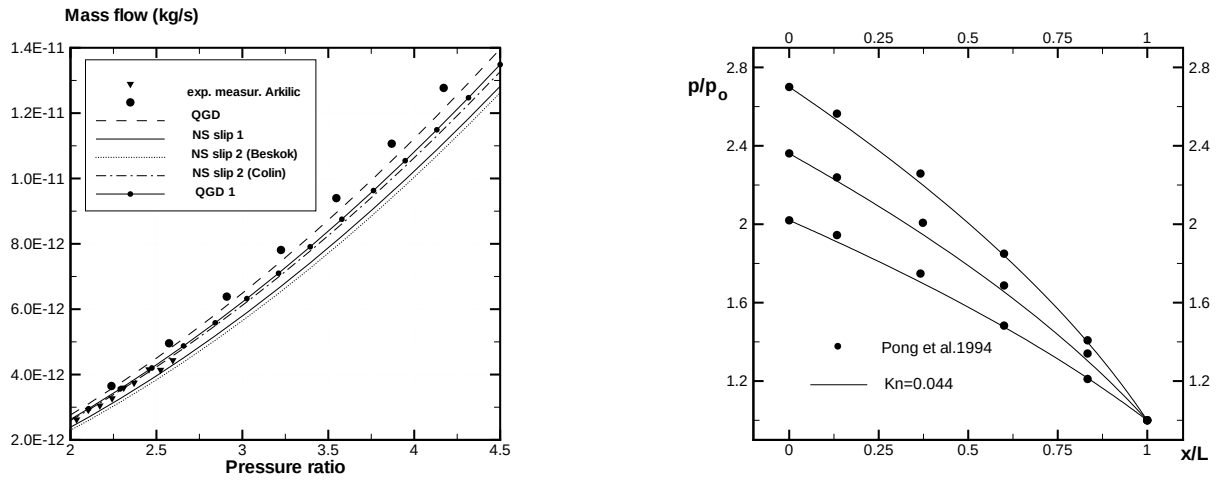

FIGURE 1. **a)** Helium mass flow in 1.33 micron height channel $Kn_o = 0.165$. The circles and triangles are the experimental measurements of [6]. The solid line with the circles presents the QGD approach (9), the solid curve is the NS solution with the first order slip condition (10), the dotted curve is the NS solution with the second order slip condition proposed by [8] (11), the dash-dotted curve is the NS solution with the second order slip boundary condition proposed by [13] (12). For all the expressions mentioned above the Chapman coefficient $k_\lambda = \sqrt{\pi/2}$ and the Maxwell value for σ_p are used. The dashed curve presents the QGD model with usual "slip parameters" $k_\lambda = A(\omega)$, $\sigma_p = 1.012$ (9). **b)** Pressure distribution in a long microchannel. The solid lines represent the analytical solutions (14) for three different pressure ratios $\mathscr{P} = 2.02, 2.36, 2.70$, the symbols are the data from [3].

The limit of the pressure gradient when $Kn \to 0$ tends toward the expression $(1-\mathscr{P}^2)/\sqrt{\mathscr{P}^2 - \tilde{x}(\mathscr{P}^2-1)}/2$ which depends on the distance $\tilde{x}$. That means that the compressibility effects remain when the rarefaction effects disappear and that, for the least, a part of the nonlinearity of the pressure distribution is due to the change in the density of the gas in the channel and not to the rarefaction effects. Otherwise, it is clear, from Fig. 2 a, that presents the deviation of the streamwise pressure from linear pressure drop, and from various numerical tests that for the large Knudsen numbers (in the frame of the continuum approach) the pressure distribution becomes, at last, linear. So, it could be deduced that the rarefaction effects serves generally to decrease the curvature in the pressure distribution caused by the compressibility effect.

Finally, let us note that expression (16) allows to obtain explicit velocity profiles (putting (16) in (5)) which, according to Fig. 2 b, agree to the numerical calculation.

CONCLUSION

We have focused our interest on the isothermal continuum approaches in the slip regime using the quasi gasdynamic equations to delimit their validity domain. From the QGD system, we have derived a mass flow rate expression and analytical profiles of pressures and velocities, using a small perturbation treatment. Up to Knudsen numbers close to 0.2 the QGD approach gives results fitting slightly better the measurements than the NS approaches (employed with first or second order slip boundary conditions). Moreover in this Knudsen range our analytical profiles agree perfectly with the "exact" QGD numerical results. In this range three main results may be pointed out:

- The QGD mass flow rate expression analytically deduced from QGD equations is similar to those obtained from the Navier-Stokes equations associated to a second order slip boundary conditions.
- The rarefaction effects reduce the curvature of the parabolic streamwise pressure profiles usually found in this Knudsen number range: when these rarefaction effects disappear $(Kn_o \to 0)$, compressibility effects remain and insure a maximal parabolic curvature to the pressure profiles.
- A change in the "slip parameters" retained for the calculations (especially a change in the choice between the slip velocity coefficients σ_p^M and σ_p^K) leads to result variations, for the least as important as those observed when changing the Knudsen number order (first or second) of the continuum approaches.

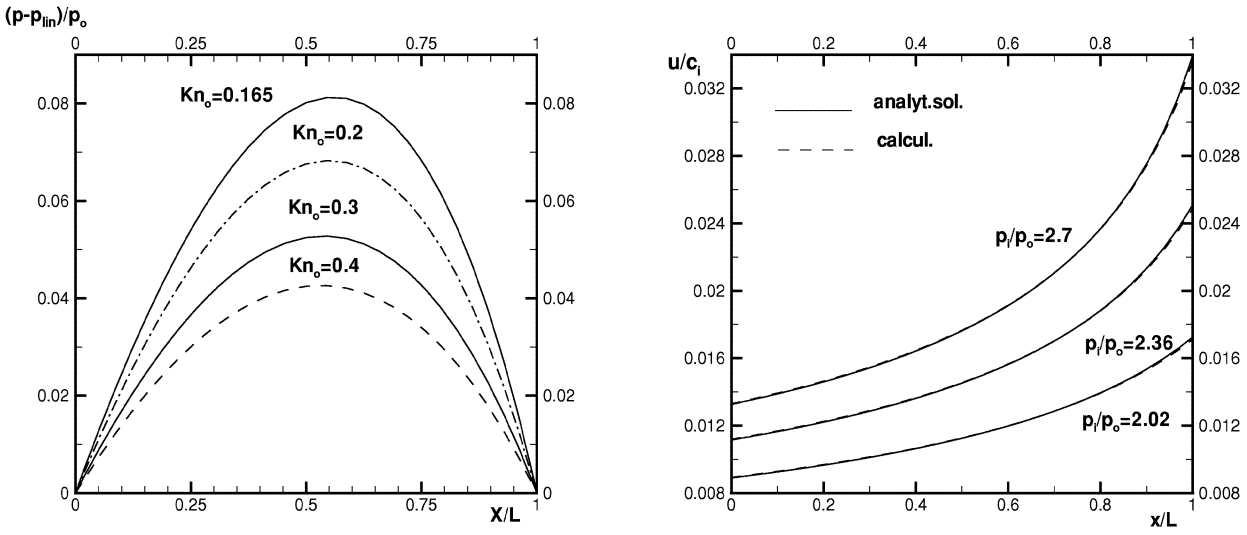

FIGURE 2. **a)** Deviation from the linear pressure drop for helium flow $\mathscr{P} = 2.36$ for the outlet Knudsen numbers $Kn_o = 0.164 \div 0.4$. **b)** Velocity variation on the channel axis for nitrogen flow, the solid line corresponds to the analytical solution, the dashed line is the numerical solution.

Calculations about more numerous experimental results and further investigations on the slip parameters (accommodation coefficients, reflection law) should clarify many questions still arrising in the microflow field.

ACKNOWLEDGMENTS

The authors gratefully acknowledge the support for this work from the National Centre of Scientific Research (CNRS), project number MI2F03-45. The authors are also thankful to Prof. T.G.Elizarova for stimulating discussions.

REFERENCES

1. Elizarova, T. G., and Sheretov, Y. V., *Computational Mathematic and Mathematical Physics*, **41**, 219–234 (2001).
2. Elizarova, T. G., and Sheretov, Y. V., *La Houille Blanche*, **5**, 66–72 (2003).
3. Pong, K. C., Ho, C. M., Liu, J., and Tai, Y. C., "Non-linear pressure distribution in uniform microchannels," in *Appl. of Microfabrication to F. Mech.*, edited by P. B. et al, Int. Mech. Eng. Cong. and Exp., ASME, 1994, vol. 197, pp. 51–56.
4. Maté, B., Graur, I. A., Elizarova, T. G., Chirokov, I. A., Tejeda, G., Fernández, J. M., and Montero, S., *Journal of Fluid Mechanics*, **426**, 177–197 (2001).
5. el Hak, M. G., *Mec. Ind.*, **2**, 313–341 (2001).
6. Arkilic, E. B., Schmidt, M. A., and Breuer, K. S., *Journal of Microelectromechanical systems*, **6**, 167–178 (1997).
7. Schlichting, H., *Boundary layer theory*, Pergamon Press, London, 1955.
8. Karniadakis, G. E., and Beskok, A., *Microflow: fundamental and simulations*, Springer-Verlag, 2002.
9. Sharipov, F., "Data on the velocity slip and temperature jump coefficients," in *Therm. and Mech. Sim. and Exp. in MEMS*, edited by L. J. E. et al, 5th Int.Conf. EuroSimE 2004, Brussels, Shaker Publishing, 2004, pp. 243–249.
10. Kogan, M. N., *Rarefied gas dynamics*, Nauka, Moscow, 1967.
11. Chapman, and Cowling, *The mathematical theory of non-uniform gases*, University Press, Cambridge, 1970, 3 edn.
12. Bird, G. A., *Molecular gas dynamics and the direct simulation of gas flows*, Oxford University Press, New York, 1994.
13. Colin, S., Lalonde, P., and Caen, R., *Heat Transfer Engineering*, **25**, 23–30 (2004).
14. Deissler, R. G., *International Journal of Heat and Mass Transfer*, **7**, 681–694 (1964).